Synthesis, Characterization, and Ligand Exchange Studies of $W_6S_8L_6$ Cluster Compounds

Song Jin, Ran Zhou, Ellen M. Scheuer, Jennifer Adamchuk, Lori L. Rayburn, and Francis J. DiSalvo*

Department of Chemistry and Chemical Biology, Baker Laboratories, Cornell University, Ithaca, New York 14853

Received November 20, 2000

Eleven organic Lewis bases were investigated as potential ligands (L) on $W_6S_8L'_6$ clusters by exploring ligand exchange reactions to form $W_6S_8L_6$ clusters. Six new homoleptic $W_6S_8L_6$ cluster complexes were prepared and characterized with L = tri-*n*-butylphosphine (P^nBu_3), triphenylphosphine (PPh_3), *tert*-butylisocyanide (^{t}BuNC), morpholine, methylamine ($MeNH_2$), and *tert*-butylamine (^{t}BuNH$_2$). While partial replacement of ligands occurred with diethylamine (Et_2NH) and dibutylamine (Bu_2NH), homoleptic clusters could not be prepared by these exchange reactions. When aniline, tribenzylamine, and tri-*tert*-butylphosphine were the potential ligands, no exchange was observed. From ligand exchange studies of these ligands and others previously studied, a thermodynamic series of binding free energies for ligands on $W_6S_8L_6$ clusters was established as the following: non-Lewis base solvents, aniline, P^tBu_3, etc. ≪ Et_2NH, Bu_2NH < ^{t}BuNH$_2$ < morpholine, piperidine ≤ ^{n}BuNH$_2$, $MeNH_2$ ≤ 4-*tert*-butylpyridine, pyridine < ^{t}BuNC < tricyclohexylphosphine (PCy_3) < PPh_3, P^nBu_3 ≤ triethylphosphine (PEt_3). Structures of the new cluster complexes were determined by X-ray crystallography. The new compounds were also characterized by NMR spectroscopy and thermogravimetric analyses (TGA). The W−L bond orders and TGA data qualitatively agree with the thermodynamic series above.

Introduction

Ever since the molecular octahedral cluster $Mo_6S_8(PEt_3)_6$ was synthesized in the late 1980s,[1] group VI octahedral chalcogenide metal clusters $M_6Q_8L_6^{2-4}$ (M = Cr,[5−7] Mo,[8−13] W;[14−23] Q = S, Se, Te; L = organic donor ligands) have attracted continued attention mainly because of their structural relationship to the well-known Chevrel phases.[24] The fascinating properties of Chevrel phases, such as superconductivity,[25,26] fast ion conductivity,[27] and catalytic activity,[28−33] motivated many attempts to prepare the Chevrel phases[10,34,35] and their unknown tungsten analogues[17−20] from these molecular precursors via low-temperature routes. We have been interested in using these molecular clusters to construct novel solid-state materials with the clusters as building blocks and π-conjugated ditopic ligands as electronically active linkers in hopes of producing materials with interesting electronic properties.[21−23,36]

* To whom correspondence to be addressed. E-mail: fjd3@cornell.edu.

(1) Saito, T.; Yamamoto, N.; Yamagata, T.; Imoto, H. *J. Am. Chem. Soc.* **1988**, *110*, 1646−1647.
(2) Saito, T. In *Early Transition Metal Clusters with π-Donor Ligands*; Chisholm, M. H., Ed.; VCH Publishers: New York, 1995.
(3) Saito, T. *Adv. Inorg. Chem* **1997**, *44*, 45−91.
(4) Prokopuk, N.; Shriver, D. F. *Adv. Inorg. Chem.* **1998**, *46*, 1−49.
(5) Hessen, B.; Siegrist, T.; Palstra, T.; Tanzler, S. M.; Steigerwald, M. L. *Inorg. Chem.* **1993**, *32*, 5165−5169.
(6) Tsuge, K.; Imoto, H.; Saito, T. *Bull. Chem. Soc. Jpn.* **1996**, *69*, 627−636.
(7) Kamiguchi, S.; Imoto, H.; Saito, T.; Chihara, T. *Inorg. Chem.* **1998**, *37*, 6852−6857.
(8) Saito, T.; Yamamoto, N.; Nagase, T.; Tsuboi, T.; Kobayashi, K.; Yamagata, T.; Imoto, H.; Unoura, K. *Inorg. Chem.* **1990**, *29*, 764−770.
(9) Hilsenbeck, S. J. Ph.D. Dissertation, Iowa State University, Ames, IA, 1993.
(10) Hilsenbeck, S. J.; Young, V. G., Jr.; McCarley, R. E. *Inorg. Chem.* **1994**, *33*, 1822−1832.
(11) Mizutani, J.; Amari, S.; Imoto, H.; Saito, T. *J. Chem. Soc., Dalton Trans.* **1998**, 819−824.
(12) Magliocchi, C.; Xie, X.; Hughbanks, T. *Inorg. Chem.* **2000**, *39*, 5000−5001.
(13) Mironov, Y. V.; Virovets, A. V.; Naumov, N. G.; Ikorskii, V. N.; Fedorov, V. E. *Chem.−Eur. J.* **2000**, *6*, 1361−1365.
(14) Saito, T.; Yoshikawa, A.; Yamagata, T. *Inorg. Chem.* **1989**, *28*, 3588−3592.
(15) Zhang, X. Ph.D. Dissertation, Iowa State University, Ames, IA, 1991.
(16) Ehrlich, G. M.; Warren, C. J.; Vennos, D. A.; Ho, D. M.; Haushalter, R. C.; DiSalvo, F. J. *Inorg. Chem.* **1995**, *34*, 4454−4459.
(17) Xie, X. B.; McCarley, R. E. *Inorg. Chem.* **1995**, *34*, 6124−6129.
(18) Zhang, X.; McCarley, R. E. *Inorg. Chem.* **1995**, *34*, 2678−2683.
(19) Xie, X. B.; McCarley, R. E. *Inorg. Chem.* **1996**, *35*, 2713−2714.
(20) Xie, X. B.; McCarley, R. E. *Inorg. Chem.* **1997**, *36*, 4665−4675.
(21) Venkataraman, D.; Rayburn, L. L.; Hill, L. I.; Jin, S.; Malik, A.-S.; Turneau, K. J.; DiSalvo, F. J. *Inorg. Chem.* **1999**, *38*, 828−830.
(22) Hill, L. I.; Jin, S.; Zhou, R.; Venkataraman, D.; DiSalvo, F. J. *Inorg. Chem.* **2001**, *40*, 2660−2665.
(23) Jin, S.; Venkataraman, D.; DiSalvo, F. J. *Inorg. Chem.* **2000**, *39*, 2747−2757.
(24) Chevrel, R.; Sergent, M.; Prigent, J. *J. Solid State Chem.* **1971**, *3*, 515−519.
(25) Chevrel, R.; Sergent, M. *Topics in Current Physics*; Fischer, Ø., Maple, M. B., Eds.; Springer-Verlag: Heidelberg, 1982; Vol. 32, Chapter 2.
(26) Pena, O.; Sergent, M. *Prog. Solid State Chem.* **1989**, *19*, 165−281.
(27) (a) Mulhern, P. J.; Haering, R. R. *Can. J. Phys.* **1984**, *62*, 527−531. (b) Aurbach, D.; Lu, Z.; Schechter, A.; Gofer, Y.; Gizbar, H.; Turgeman, R.; Cohen, Y.; Moshkovich, M.; Levi, E. *Nature* **2000**, *407*, 724−727.
(28) McCarty, K. F.; Anderegg, J. W.; Schrader, G. L. *J. Catal.* **1985**, *93*, 375−387.
(29) Kareem, S. A.; Miranda, R. *J. Mol. Catal.* **1989**, *53*, 275−283.
(30) Hilsenbeck, S. J.; McCarley, R. E.; Thompson, R. K.; Flanagan, L. C.; Schrader, G. L. *J. Mol. Catal. A: Chem.* **1997**, *122*, 13−24.
(31) Hilsenbeck, S. J.; McCarley, R. E.; Goldman, A. I.; Schrader, G. L. *Chem. Mater.* **1998**, *10*, 125−134.
(32) Paskach, T. J.; Hilsenbeck, S. J.; Thompson, R. K.; McCarley, R. E.; Schrader, G. L. *J. Alloys Compd.* **2000**, *311*, 169−180.
(33) Thompson, R. K.; Hilsenbeck, S. J.; Paskach, T. J.; McCarley, R. E.; Schrader, G. L. *J. Mol. Catal. A: Chem.* **2000**, *161*, 75−87.
(34) Hilsenbeck, S. J.; McCarley, R. E.; Goldman, A. I. *Chem. Mater.* **1995**, *7*, 499−506.
(35) McCarley, R. E.; Hilsenbeck, S. J.; Xie, X. *J. Solid State Chem.* **1995**, *117*, 269−274.
(36) Malik, A.-S. Ph.D. Thesis, Cornell University, Ithaca, NY, 1998.

10.1021/ic001314q CCC: $20.00
Published on Web 05/04/2001

Table 1. Designations of the $W_6S_8L_6$ Clusters *n* and Abbreviations and Properties of Ligands L

ligand L	abbreviation	*n*	bp/°C	pK_a [a]	C_B/E_B [b]
tri-*n*-butylphosphine	P^nBu_3	**1**	150/50 mmHg	8.43	5.36/0.32
triphenylphosphine	PPh_3	**2**	377(80)	2.73	3.05/0.70
tert-butylisocyanide	^{t}BuNC	**3**	91	−	−
morpholine	Morph	**4**	129	8.33	−
methylamine	$MeNH_2$	**5**	−6.3	10.657	3.12/2.16
tert-butylamine	^{t}BuNH$_2$	**6**	46	10.83	−
triethylphosphine	PEt_3	**7**[14,21]	127	8.69	5.53/0.28
tricyclohexylphosphine	PCy_3	**8**[23]	82 (mp)	9.70	5.35/0.41
4-*tert*-butylpyridine	4-tbp	**9**[16]	196	6.0	3.64/1.90[c]
pyridine	py	**10**[16,18]	115	5.25	3.54/1.78
piperidine	pip	**11**[21,15]	106	11.123	4.93/1.44
tetrahydrothiophene	THT	**12**[15]	119	−	4.07/0.26
n-butylamine	^{n}BuNH$_2$	**13**[21]	78	10.77	3.30/2.34[c]
diethylamine	Et_2NH		55	10.489	4.54/1.22
di-*n*-butylamine	Bu_2NH		159	−	−
aniline			184	4.63	−
tribenzylamine			91 (mp)	−	5.73/1.32[c]
tri-*tert*-butylphosphine	P^tBu_3		102/13 mmHg	−	6.08/0.25

[a] pK_a values mostly in 25 °C aqueous solutions. Taken from refs 40 and 41 for amines and ref 42 for phosphines. [b] C_B and E_B values are covalent and electrostatic parameters, respectively, characteristic of Lewis bases defined by Drago. Listed values are the most recent versions, taken from ref 43 for phosphines and ref 44 for others. [c] The data for their close anologues are given: 4-ethylpyridine for 4-tbp, ethylamine for ^{n}BuNH$_2$, $(C_2H_5)_3N$ for tribenzylamine. "−" means the data are not available.

Conceptually, such extended cluster networks can be made by replacing the monodentate ligands (L) on the $M_6Q_8L_6$ cluster with ditopic ligands. These targets are analogous to the numerous compounds reported by supramolecular inorganic chemists[37−39] except that here the octahedral clusters replace single metal ions in those networks. In practice, the knowledge of the axial coordination chemistry of the clusters, in contrast to the well-established coordination chemistry of single metal complexes, has been insufficient to allow the implementation of such simple concepts in a rational fashion. A number of group VI $M_6Q_8L_6$ (M = Cr, Mo, W; Q = S, Se, Te) clusters have been reported with the following ligands: triethylphoshine (PEt_3),[1,5,8,14,21] tricyclohexylphosphine (PCy_3),[23] pyridine (py),[10,16−20] 4-*tert*-butylpyridine (4-tbp),[16,21] piperidine (pip),[10,15,17,21] pyrrolidine,[9] propylamine,[10] *n*-butylamine (^{n}BuNH$_2$),[23] and tetrahydrothiophene (THT).[15] Those bound to W_6S_8 clusters are designated in Table 1. However, the focus was often the construction of the cluster compounds, while little attention was paid to the interconversions between them. Driven by our goal of constructing networks of W_6S_8 clusters via axial ligand exchange reactions, we extensively studied many organic donor compounds as potential ligands to the W_6S_8 clusters (listed in Table 1) and systematically compared the thermodynamics of ligand binding to the clusters. Our findings are reported here. Six new $W_6S_8L_6$ cluster complexes, **1**−**6** (designated in Table 1), were synthesized through ligand exchange reactions and characterized by X-ray crystallography. These new complexes, along with those reported previously, were examined with quantitative or qualitative NMR spectroscopy, thermogravimetric analyses, and structure analyses when available in an attempt to develop a thermodynamic scale of binding free energy.

Experimental Section

General. Cluster complexes **9**, **11**, and **13** were synthesized according to reported procedures.[21,23] All other reagents were of commercial origin. Acetonitrile was dried with 4 Å molecular sieves. Morpholine, *n*-butylamine, dibutylamine, diethylamine, and aniline were dried with potassium hydroxide, degassed, and distilled under reduced pressure. THF, diethyl ether, and benzene were treated with sodium wire and distilled under reduced pressure. All others were used as received. Methylamine solution in THF, *tert*-butylamine, and *tert*-butylisocyanide were received sealed under dinitrogen from Aldrich. Deuterated benzene (sealed under dinitrogen) was purchased from Cambridge Isotope Laboratories, Inc. All reagents and products were stored in a glovebox filled with argon. All operations were carried out in the glovebox unless otherwise stated. The "reaction bomb" used below is a thick-walled glass vessel (i.d. = 1 in., thickness = $^1/_8$ in.) equipped with a Teflon valve and a Teflon stir bar.

^{1}H and ^{13}C NMR spectra were obtained using an IBM/Bruker AF-300 instrument or a Varian VXR-400 instrument and were internally referenced to residual solvent resonance. ^{31}P NMR spectra were obtained using a Varian VXR-400 instrument at 162 MHz with 85% H_3PO_4 as an external standard and with ^{1}H decoupling unless otherwise noted. Powder X-ray diffraction was done on a Scintag XDS2000 diffractometer. FT-IR spectrum was collected with KBr pellet on a Mattson Polaris spectrometer equipped with a 4326 upgraded electronics package and a DTGS detector.

Synthesis of $W_6S_8(P^nBu_3)_6$ (1). A reaction bomb was charged with W_6S_8(4-tbp)$_6$ (**9**) (0.500 g, 0.230 mmol) and P^nBu_3 (0.326 g, 1.61 mmol) along with 20 mL of THF and was brought out of the glovebox. After the mixture was heated to 100 °C for 24 h, the solvent was removed in dynamic vacuum. The solid residue was washed with acetonitrile, dried in vacuo, and weighed (0.520 g, 88% yield). As prepared, this solid contained X-ray quality crystals.

This compound is very soluble in THF and benzene, soluble even in Et_2O and heptane, but insoluble in acetonitrile. ^{1}H NMR in C_6D_6: δ 2.1−2.05 (broad, α-H, 2), 1.88−1.76 (broad, β-H, 2), 1.55 (sextet, γ-H, 2), 1.05 (t, Me, 3), ^1J = 7 Hz. ^{31}P{^{1}H} NMR: δ −24.44; satellite peaks (broad), −23.65 to −23.75, −25.14 to −24.24, $^1J_{w-p}$ = 240 Hz.

Synthesis of $W_6S_8(PPh_3)_6$ (2). Cluster **9** (0.200 g, 0.0918 mmol) and PPh_3 (0.169 g, 0.645 mmol) were sealed in a reaction bomb along with 10 mL of benzene. The vessel was brought out of the glovebox and heated to 100 °C for 48 h. The initial slurry became a dark-red clear solution and then became a slurry again. The light orange-red fine precipitate was filtered, washed with benzene, dried in vacuo, and weighed (0.169 g, 63% yield). Some block-shaped red crystals suitable for X-ray analysis could be found in the product. This compound is insoluble in common solvents.

Synthesis of $W_6S_8(^t$BuNC$)_6$ (3). A reaction bomb was charged with **9** (0.194 g, 0.089 mmol) and *tert*-butylisocyanide (0.089 g, 1.07 mmol) along with 2.5 g of benzene and brought out of the glovebox. After 3 days at 100 °C in an oil bath, X-ray quality brown-red crystals

(37) Lehn, J.-M. *Pure Appl. Chem.* **1994**, *66*, 1961−1966.
(38) Lehn, J.-M. *Supramolecular Chemistry*: *Concepts and Perspectives*; VCH: Weinheim, Germany, 1995.
(39) Zaworotko, M. J. In *Crystal Engineering*: *The Design and Application of Functional Solids*; Seddon, K. R., Zaworotko, M., Eds.; NATO Science Series C, Vol. 539; Kluwer Academic: Dordrecht, The Netherlands, 1999.

Table 2. ^{1}H NMR Chemical Shifts (ppm) for Heteroleptic $W_6S_8(LL')_6$ Cluster Complexes (L = 4-tbp and L′ = Amines)

		^{1}H NMR chemical shifts in C_6D_6				
		bound 4-tbp			bound amine	
W_6S_8(4-tbp)$_6$ g (mmol)	amine g (mmol) (cluster/amine)	*o*-H multiple peaks	*m*-H multiple peaks	Me multiple singlets	H on N	alkyl H
0.400 (0.184)	*tert*-butylamine 4.0 (55) (1:300)	9.83−9.77	6.65−6.62	0.77−0.72	3.81, 3.77, 3.73, 3.69 (singlets)	1.30, 1.28, 1.26, 1.24 (all singlets, Me)
0.200 (0.0918)	diethylamine 3.06 (41.9) (1:450)	9.88−9.80	6.68−6.62	0.79−0.76	3.9−3.8 (broad)	3.41−3.34 (multiplets, α-H), 1.16−1.08 (multiplets, Me)
0.115 (0.0530)	dibutylamine 2.82 (21.9) (1:410)	9.82−9.65	6.63−6.57	0.78−0.69	3.9−3.6 (broad)	3.3−3.1 (broad, α-H), 1.7−1.2 (two broad humps, rest)

precipitated from solution upon slow cooling. These crystals were collected by filtration in a glovebox, washed with Et_2O, and weighed when dry (0.094 g, 57% yield).

This compound is very soluble in acetonitrile, moderately soluble in benzene, slightly soluble in THF, and insoluble in Et_2O and heptane. ^{1}H NMR in C_6D_6: δ 0.694 (s, Me). IR: 2135 cm^{-1} (ν_{CN}).

Synthesis of W_6S_8(morp)$_6$ (4). A reaction bomb was charged with **9** (0.223 g, 0.106 mmol) and morpholine (0.936 g, 10.61 mmol) and then was brought out of the glovebox and heated to 100 °C for 2 days. The brownish yellow solid precipitate was filtered, then washed with Et_2O. The dried product weighed 0.105 g (54% yield).

Cluster **4** is somewhat soluble in aniline, slightly soluble in DMF, sparingly soluble in THF, benzonitrile, and acetonitrile, and insoluble in other common solvents. Single crystals were grown by vapor diffusion of Et_2O into an aniline/morpholine solution of **4**.

Synthesis of $W_6S_8(MeNH_2)_6$ (5). $W_6S_8(^nBuNH_2)_6$ (**13**) (0.400 g, 0.222 mmol) was dissolved in 4 mL of benzene in a reaction bomb, and a 2.0 M solution of methylamine in THF (12.0 mL, 24.0 mmol) was added. Then the reaction bomb was brought out of the glovebox and heated to 100 °C for 4 days. The black precipitate was filtered, washed with Et_2O, and weighed (0.277 g, 80% yield). *Caution:* Heating methylamine solutions in closed containers can generate high pressure.

Cluster **5** is soluble in aniline and DMF, slightly soluble in THF and CH_2Cl_2, and insoluble in other common solvents. Single crystals were grown by vapor diffusion of Et_2O into an aniline solution of **5**.

Synthesis of $W_6S_8(^tBuNH_2)_6$ (6). $W_6S_8(^nBuNH_2)_6$ (0.200 g, 0.111 mmol) and 3.0 mL of *tert*-butylamine (28 mmol) were sealed in a reaction bomb to form a brown-red solution. The vessel was taken out of the glovebox and heated at 100 °C for 48 h without a change in the appearance of the solution. The solution was then layered with acetonitrile (10 mL) to yield a flaky precipitate in a few days, which was filtered and washed with acetonitrile and Et_2O. The product weighed 0.105 g (53% yield).

Single crystals were grown by layering acetontrile on top of a *tert*-butylamine solution of **6**. ^{1}H NMR in C_6D_6: δ 3.69 (s, H on N, 2), 1.25 (s, Me, 9). ^{13}C NMR in C_6D_6: δ 53.7 (*tert*-C), 31.0 (Me).

Ligand Exchange Reactions with Other Amines. Typical reactions were carried out in reaction bombs with W_6S_8(4-tbp)$_6$ and excess neat amines as the solvent. The initial red slurries became brown-red solutions after they were heated at 100 °C for 2 days. After the solvents were removed under dynamic vacuum, ^{1}H NMR in C_6D_6 were recorded on the amorphous products. The reactions and the chemical shifts are listed in Table 2.

Using Quantitative ^{1}H NMR To Monitor the Exchange Reactions. Ligand exchange reactions were monitored with quantitative ^{1}H NMR. The starting clusters and stock solutions of the incoming ligands in C_6D_6 together with comparable amounts of pentamethylbenzene were loaded into threaded NMR tubes (5 mm o.d. from Kontes, Inc.) and sealed with caps lined with Teflon septa. The NMR tubes were taken out of the glovebox and heated in an oil bath at 100 °C. Free induction decay NMR spectra were taken at room temperature before and after the reactions with 60 s delay times ($>5T_1$ for the protons with longest T_1) to detect all the ^{1}H spins. The mole ratios of the ligands were determined from the peak integral ratios in the NMR spectra. The details and the results are given in Table 3.

Table 3. Progress of Ligand Substitution of L with L′ on $W_6S_8L_6$ Clusters Derived from Quantitative ^{1}H NMR[a]

before reactions			after equilibrium
cluster $W_6S_8L_6$	ligand L′	ratio L/L′	ratio L bound/unbound[b]
W_6S_8(4-tbp)$_6$	pip	6:13	3.0:3.0
	pip	6:18	1.3:4.7
	pip	6:21	1.1:4.9[c]
	pip	6:210	nearly complete
	morph	6:62	1.0:5.0[c]
	^{n}BuNH$_2$	6:10	1.8:4.2
	^{n}BuNH$_2$	6:18	1.2:4.8
	^{n}BuNH$_2$	6:26	0.42:5.58
	^{n}BuNH$_2$	6:100	nearly complete
	^{t}BuNH$_2$	6:11	3.4:2.6
	^{t}BuNH$_2$	6:70	1.6:4.4
	Bu$_2$NH	6:90	4.8:1.2
	Et$_2$NH	6:78	2.6:3.4
W_6S_8(pip)$_6$	4-tbp	13:8	3.0:3.0
	4-tbp	13:69	5.0:1.0
	^{n}BuNH$_2$	6:2.9	3.9:2.1
	^{n}BuNH$_2$	6:7.2	2.6:3.4
	^{n}BuNH$_2$	6:11.5	2.2:3.8

[a] The reactions were run in sealed NMR tubes at 100 °C for 24 h with C_6D_6 as solvent. The ratios were determined with integrals from quantitative NMR spectra taken at room temperature before and after reactions. [b] Expressed in mole ratios of ligands with a sum of 6. [c] Some precipitate was observed after the reaction, which could be due to the reduced solubility of the product in C_6D_6.

X-ray Structure Determination. Single crystals suitable for X-ray crystallographic analyses were obtained for clusters **1**−**6**, as described in the synthesis section. Crystals were mounted on a thin plastic loop using polybutene oil and were immediately cooled in a cold dinitrogen stream. Single-crystal X-ray diffraction data were collected on a Bruker SMART system with a CCD detector using Mo Kα radiation at 173 K. The cell constants were determined from more than 50 well-centered reflections. The data were integrated using SAINT software,[45] and empirical absorption corrections were applied using the SADABS program or the β revision.[46] The space groups were determined on the basis of systematic absences, intensity statistics, and the successful

(40) Perrin, D. D. *Dissociation Constants of Organic Bases in Aqueous Solution*; Butterworth: London, 1965.
(41) Lide, D. R. *CRC Handbook of Chemistry and Physics*, 74th ed.; CRC Press: Boca Raton, FL, 1993.
(42) McAuliffe, C. A.; Levason, W. *Phosphine, Arsine and Stibine Complexes of the Transition Elements*; Elsevier Scientific Publishing Company: New York, 1979; p 70.
(43) Drago, R. S.; Dadmun, A. P.; Vogel, G. C. *Inorg. Chem.* **1993**, *32*, 2473−2479.
(44) Joerg, S.; Drago, R. S.; Sales, J. *Organometallics* **1998**, *17*, 589−599.
(45) *SAINT Plus: Software for the CCD Detector System*; Bruker Analytical X-ray System: Madison, WI, 1999.
(46) Sheldrick, G. M. *SADABS* (the computer program SADABS is used by Siemens CCD diffractometers); Institute für Anorganische Chemie der Universität Göttingen: Göttingen, Germany, 1999.

Table 4. Crystallographic Data for 1, **2**·C_6H_6, **3**·4C_6H_6, **4**·3.7(aniline)·1.3(morph), **5**, and **6**·2^{t}BuNH$_2$[a]

	1	**2**·C_6H_6	**3**·4C_6H_6	**4**·3.7(aniline)·1.3(morph)	**5**	**6**·2^{t}BuNH$_2$
chemical formula	$C_{72}H_{162}P_6S_8W_6$	$C_{114}H_{96}P_6S_8W_6$	$C_{54}H_{78}N_6S_8W_6$	$C_{51.5}H_{91.5}N_{11}O_{7.25}S_8W_6$	$C_6H_{30}N_6S_8W_6$	$C_{32}H_{88}N_8S_8W_6$
fw	2573.42	3011.31	2170.80	2340.44	1545.94	1944.68
space group	*C*2/*c* (No. 15)	$P\bar{1}$ (No. 2)	$P\bar{1}$ (No. 2)	*C*2/*c* (No. 15)	$P\bar{1}$ (No. 2)	*C*2/*c* (No. 15)
a, Å	24.6648(12)	14.6107(6)	12.1751(6)	14.8105(13)	9.0847(5)	23.1036(4)
b, Å	19.8619(9)	16.6282(7)	12.5456(6)	18.5419(17)	9.1602(5)	20.8216(3)
c, Å	20.1365(10)	21.2344(9)	12.7678(6)	25.108(2)	9.5660(5)	11.497
α, deg		96.3869(9)	111.5324(11)		103.7320(10)	
β, deg	103.3240(10)	93.7166(10)	110.3392(11)	104.284(2)	116.6220(10)	99.7030(10)
γ, deg		92.1225(10)	93.1387(11)		106.2650(10)	
V, Å^3	9599.1(8)	5111.0(4)	1663.41(14)	6681.8(10)	619.10(6)	5451.46(12)
Z	4	2	1	4	1	4
T, °C	−108(2)	−100(2)	−108(2)	−108(2)	−100(2)	−108(2)
ρ_{calcd}, g cm^{-3}	1.781	1.957	2.167	2.327	4.147	2.369
μ, cm^{-1}	74.69	70.31	106.19	105.93	284.38	129.46
R_1 [b] (I > 2σ/all)	0.0250/0.0396	0.0368/0.0723	0.0412/0.0693	0.0304/0.0389	0.0444/0.0470	0.0325/0.0465
wR_2 [c] (I > 2σ/all)	0.0506/0.0590	0.0767/0.0881	0.0823/0.0910	0.0595/0.0613	0.1222/0.1239	0.0747/0.0905

[a] Determined using Mo Kα radiation (λ = 0.710 73 Å). [b] $R_1 = \sum||F_o| - |F_c||/\sum|F_o|$. [c] $wR_2 = [\sum w(F_o^2 - F_c^2)^2/\sum w(F_o^2)^2]^{1/2}$.

refinements of the structures. The structures were solved using SHELXS[47] with direct methods (all except **5**) or the Patterson method (**5**) to reveal the positions of W and S atoms. Difference Fourier syntheses following the subsequent full-matrix least-squares refinements on F_o^2 with SHELXL software packages[47] revealed the ligand atoms. Hydrogen atoms were assigned to the ideal positions and refined using a riding model. There was some disorder in the butyl groups of the ligand in cluster **1** and in a phenyl group of a ligand in cluster **2**, which was modeled successfully. In the crystal structure of **4**, a disordered solvent molecule position was found to be partially occupied by both morpholine and aniline, and the occupancy of morpholine was about 0.65 by refinement. All nonsolvent non-hydrogen atoms were refined anisotropically. All final refinements converged, and the residual electron densities were near the W atoms (typically within 1 Å). The crystallographic data are listed in Table 4. Cluster **6** was also found to crystallize in space group $P\bar{3}1c$ (No. 163) with a = 11.9404(5) Å and c = 18.7155(7) Å, without any solvents of crystallization. Because of the poor quality of the data, we were not able to refine the structure to an acceptable R value.

Thermogravimetric Analysis (TGA). The thermogravimetric analyses (TGA) of the cluster complexes were done on a Seiko TG/DTA 220 thermal analyzer. The samples were loaded onto an aluminum pan and were heated from room temperature to 550 °C at a rate of 20 °C/min under a flow of dinitrogen (60 mL/min).

Results and Discussion

Although the clusters reported herein were not previously known, the inner core of the W_6S_8 clusters are known to be rather robust, while the axial ligands are usually labile above room temperature. In section A, these ligands (listed in Table 1) are discussed in three categories according to their exchange behavior: (i) those that can completely replace existing ligands and with which new $W_6S_8L_6$ cluster complexes were synthesized; (ii) those that can only partially replace existing ligands and with which homoleptic $W_6S_8L_6$ clusters were not isolated; (iii) those with which no ligand exchange occurred. The new $W_6S_8L_6$ clusters from class i were subject to X-ray structural analyses and TGA studies, as presented in sections B and C. When homoleptic clusters could not be prepared, thermodynamic information could still be extracted from the ligand exchange reactions using quantitative NMR and other techniques. On the basis of these observations, the ligands listed in Table 1 are compared from thermodynamic and kinetic perspectives.

A. Ligand Exchange Reactions of $W_6S_8L_6$ Clusters. i. Syntheses of New Homoleptic Clusters 1−6 and Their Properties. Because its synthesis in high yield and quantity is routine in our hands,[21] the W_6S_8(4-tbp)$_6$ cluster is the starting material for the preparation of other W_6S_8 compounds. Among the new clusters, **1**−**5** could be synthesized by directly replacing 4-tbp with the incoming ligand at 100 °C. For ligands P^{n}Bu$_3$, PPh$_3$, and ^{t}BuNC, somewhat greater than the needed 6 equiv of the new ligands per cluster are sufficient to ensure complete replacement of the 4-tbp. For morpholine and methylamine, a large excess (several hundred equivalents) of ligand is essential for complete exchange. At fewer equivalents, only partial replacement occurred as shown by ^{1}H NMR, in which the characteristic resonances of bound and unbound 4-tbp ligand are clearly discerned. For *tert*-butylamine, even a large excess of neat ligand (300 equiv) cannot fully replace the 4-tbp. However, when W_6S_8(^{n}BuNH$_2$)$_6$ is used as the precursor, excess neat *tert*-butylamine is capable of completely replacing the ^{n}BuNH$_2$ ligands, enabling the synthesis of the new cluster **6**. The reported synthesis for cluster **5** was also convenient through this route. The synthetic routes and interconversions of these clusters are summarized in Figure 1.

The identities of the new clusters were confirmed by X-ray structural analyses (vide infra). For routine study, ^{1}H NMR is a good technique to verify the completeness of the ligand exchange and to characterize the new cluster complexes provided that the products are soluble in available deuterated solvents, as for **1**, **3**, and **6**. The ^{1}H NMR spectra display signals from the bound ligands, which are generally shifted downfield because of the electron-withdrawing effect of the coordination to the W atoms. Once assigned, the signals can be used to evaluate the results of the ligand exchange reactions. The powder diffraction pattern of **5** matches the simulated powder pattern from its single-crystal structure (Figure S1 in Supporting Information). The characteristic ν(CN) band observed for compound **3** (2135 cm^{-1}) is shifted just slightly lower than the ν(CN) band in unbound ^{t}BuNC (2138 cm^{-1}), which indicates a very weak π back-bonding between the W atoms and the ligands.[48] This is consistent with the structural analysis (vide infra).

Like PEt$_3$,[21] the ligands P^{n}Bu$_3$ and PPh$_3$ completely replace 4-tbp at slightly more than 1:6 ratios (cluster/ligand), which demonstrates that they are thermodynamically more favorable

(47) Sheldrick, G. M. *SHELXL*, version 5.10; Siemens Analytical X-ray Instruments, Inc.: Madison, WI, 1999.

(48) Nakamoto, K. *Infrared and Raman Spectra of Inorganic and Coordination Compounds*, 5th ed.; Wiley: New York, 1997.

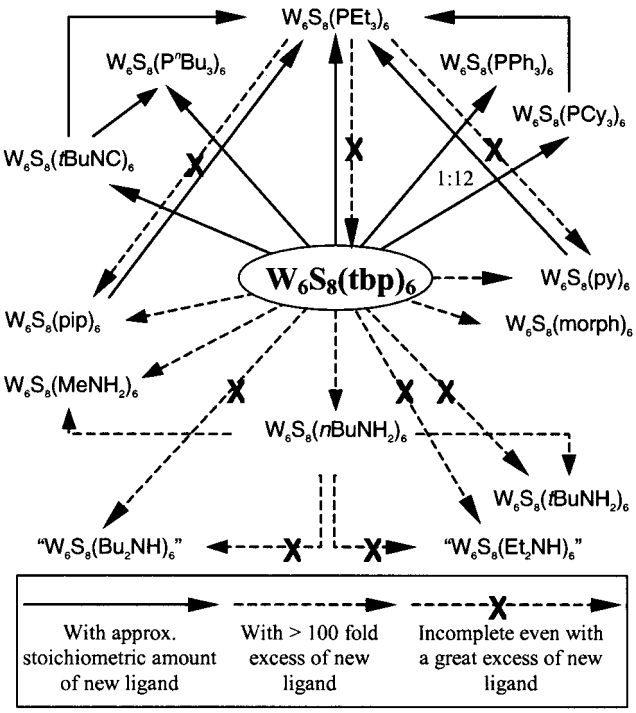

Figure 1. Summary of interconversions of $W_6S_8L_6$ complexes via ligand exchange. The different arrows, as explained in the bottom legend box, represent experimental results. Some reactions are omitted because of presentation difficulty.

ligands on W_6S_8 clusters than 4-tbp. The exchange reactions between these phosphine clusters showed that P^nBu_3 is slightly less favorable than PEt_3. However, $W_6S_8(P^nBu_3)_6$ is more soluble in a wider variety of solvents than $W_6S_8(PEt_3)_6$.[21] Because cluster **2** is not soluble, detailed comparisons of PPh_3 with other phosphines were not obtained.

Isocyanides represent a new class of ligands for W_6S_8 clusters, where ligand coordination is through the C atoms of R—N≡C. On the basis of its exchange behavior, ^{t}BuNC is more tightly bound than 4-tbp but less tightly bound than phosphines. The strong ligation of ^{t}BuNC to the cluster suggests that ditopic aromatic isocyanide ligands, such as 1,4-phenylene diisocyanide, could be useful for building linked networks.

Morpholine was chosen for study because of its similarity to piperidine[21] and the possible influence of the oxygen on the ligand binding strength when compared to piperidine. Unfortunately, **4** is not very soluble in common solvents, which makes it less useful to us. No detailed comparisons between morpholine and piperidine clusters were attempted, though they appear to bind with similar strength. Methylamine deserves some extra attention because it has the smallest volume of the ligands studied. This might allow faster kinetics in the ligand exchange using this amine. Also because of its small volume, its solubility is greatly reduced from those of other clusters with alkylamine ligands. However, aniline is a good solvent, perhaps because of hydrogen bonding to the bound methylamines.

The $W_6S_8(^t BuNH_2)_6$ compound seems to be less stable than $W_6S_8(^n BuNH_2)_6$.[23] The solid compound degraded with time after it was isolated from the mother liquor, as evidenced by the more complicated NMR spectra and reduced solubility. The different behavior of the *tert*-butylamine and *n*-butylamine is not likely due to different basicity because the pK_a values of these two primary amines are very close (10.77 for $^n BuNH_2$ and 10.83 for $^n BuNH_2$).[41] It is likely that steric hindrance is responsible; the bulky *tert*-butyl group may have repulsive interactions with the S atoms on the clusters.

ii. Partial Ligand Exchange Reactions. When an excess (>400 equiv) of neat diethylamine or dibutyalmine was used to react with W_6S_8(4-tbp)$_6$, the products were mixtures of heteroleptic clusters coordinated by both 4-tbp and amine ligands as evidenced by multiple peaks (9.65−9.88, 6.57−6.68 ppm and those at 1−4 ppm) in ^{1}H NMR spectra. These correspond to the bound ligands on the clusters (see Table 2). The two groups of aromatic peaks were slightly shifted upfield from those of the bound 4-tbp in **9**, and the groups of peaks at 1−4 ppm were slightly shifted downfield from those of the unbound amines. The peaks from protons on and close to the amine N atoms were often broad, which indicates the dynamic nature of these W−N bonds.[49] When $W_6S_8(^n BuNH_2)_6$ was used as precursor, NMR spectra of the green residues resulting from the removal of the free ligand were complicated and did not match the expected spectra of homoleptic cluster complexes. For the case of diethylamine, some portion of this greenish residue could not be redissolved in any solvent. We conclude that if such clusters as $W_6S_8(R_2NH)_6$ exist, they are not stable without excess ligand present. Therefore, these dialkylamine compounds are even less stable than the $^t BuNH_2$ compound. The difference between these secondary amines and *cyclic* secondary amines could perhaps be explained by steric interactions between the respective ligand and the cluster. Such repulsion should be less severe for *cyclic* secondary amines because of the ring restriction. We speculate that direct intercluster W−S linkages such as those present in Chevrel phases[24] occur when the ligands are weakly bound and labile, leading to sometimes insoluble products. Such direct intercluster linkage, as observed in the Chevrel-like cluster dimer $Mo_{12}S_{16}(PEt_3)_{10}$ by Saito and co-workers,[50] is a competing reaction pathway to ligand exchange. This hypothesis was also the basis for McCarley and co-workers' attempts to make tungsten analogues of Chevrel phases by removing labile ligands, especially amine ligands, from clusters at low temperature.[17−20]

iii. Other Potential Ligands Investigated. Other potential candidates were not found to ligate the W_6S_8 cluster at all. The basicity of aniline (pK_a = 4.63)[41] is greatly reduced in comparison to other amines by the π delocalization of the lone pair electrons. Aniline was not found to bind to the W_6S_8 cluster in ligand exchange attempts with cluster **9** or even **13** as monitored with NMR. However, it has been found to be a universal solvent for many known $W_6S_8L_6$ compounds. Not surprisingly, the very bulky tertiary amine, tribenzylamine, also did not bind to different W_6S_8 clusters in reactions monitored by NMR. While all other phosphines are good ligands, the fact that P^tBu_3 does not bind to the cluster at all is rather surprising. This is likely explained by steric hindrance; P^tBu_3 has a large Tolman cone angle (182°).[51]

iv. Monitoring the Ligand Exchanges: NMR Tube Reactions. The results of quantitative NMR reactions are listed in Table 3. We were able to calculate the progress of ligand replacement with peak integrals of bound and unbound ligands (estimated relative error at 2σ: 10%). These data help compare the less strongly bound amine ligands with each other. The difference between these amines is quite small based on these results. Nevertheless, the distinction between acyclic secondary amines and primary amines is quite clear. Also, the difference between $^t BuNH_2$ and $^n BuNH_2$ confirms the previous qualitative observations. By strict comparison of ratios, $^n BuNH_2$ is a more

(49) Cotton, F. A.; Dikarev, E. V.; Herrero, S. *Inorg. Chem.* **1999**, *38*, 2649−2654.
(50) Amari, S.; Imoto, H.; Saito, T. *Chem. Lett.* **1997**, 967−968.
(51) Tolman, C. A. *Chem. Rev.* **1977**, *77*, 313−348.

Table 5. Selected Interatomic Distances [Å] and Bond Angles [deg] for $W_6S_8L_6$ Clusters

	clusters L					
	P^nBu_3	PPh_3	^{t}BuNC	morpholine	$MeNH_2$	^{t}BuNH$_2$
W−W	2.6737(2)−2.6788(2)	2.6749(4) − 2.6899(4)	2.6776(5)−2.6870(5)	2.6563(3)−2.6687(3)	2.6493(7)−2.6714(7)	2.6577(4)−2.6680(4)
mean[a]	2.676(2)	2.683(4)	2.681(3)	2.662(5)	2.661(8)	2.664(3)
δ_{w-w}[b]	0.0051	0.015	0.0094	0.0124	0.0221	0.0103
W−S	2.4522(7)−2.4647(7)	2.4262(18) −2.4692(19)	2.443(2)−2.456(2)	2.4493(11)−2.4676(12)	2.436(3)−2.481(3)	2.443(2)−2.477(2)
mean[a]	2.458(4)	2.449(12)	2.450(5)	2.458(5)	2.462(15)	2.464(9)
δ_{w-s}[b]	0.0125	0.043	0.013	0.0183	0.045	0.034
W−W−W[c]	89.970(6)−90.029(6)	89.619(13)−90.383(13)	89.896(15)−90.105(15)	89.862(9)−90.139(10)	89.98(2)−90.02(2)	89.804(12)−90.196(12)
δ_{w-w-w}[b]	0.059	0.764	0.209	0.277	0.04	0.392
W−W−W[d]	59.918(4)−60.092(4)	59.737(11)−60.291(11)	59.882(13)−60.151(14)	59.720(7)−60.179(8)	59.553(18)−60.296(17)	59.793(11)−60.175(11)
δ_{w-w-w}[b]	0.174	0.554	0.269	0.459	0.743	0.382
W−L	2.5172(8)−2.5202(8)	2.5561(19)−2.5915(19)	2.146(9)−2.169(9)	2.303(4)−2.313(4)	2.265(10)−2.293(9)	2.292(6)−2.311(6)
mean[a]	2.518(1)	2.570(12)	2.160(10)	2.307(4)	2.278(11)	2.303(8)
L−L	6.138−6.336	6.051−6.581	5.590−5.863	5.812−6.034	5.724−6.038	5.576−6.234
δ_{L-L}	0.198	0.530	0.273	0.222	0.314	0.658

[a] Followed by standard deviations (σ's) of the group of bond lengths in parentheses. $\sigma = \{\sum(d_j - d_m)^2/n\}^{1/2}$. [b] Maximum deviations. [c] Within equatorial squares. The mean W−W−W angles within the equatorial squares are automatically 90° if the clusters have inversion centers. For cluster complex $W_6S_8(PPh_3)_6$, the observed mean is 90.00(1)°. [d] Within triangular faces. The mean angles are 60° by geometry.

favorable ligand on the W_6S_8 cluster than piperidine, though the difference is just within experimental error.

In summary, with the information presented above, we can now compare the binding thermodynamics of these ligands. The ligand exchange reactions are a probe of the relative thermodynamics of ligand binding on the W_6S_8 cluster in *solution phases*. A thermodynamic ligand binding series can thus be established as the following:

non-Lewis base solvents, aniline, P^tBu_3, etc. ≪

$$Et_2NH,\ Bu_2NH < {}^t\text{BuNH}_2 < \text{morpholine, pip} \leq {}^n\text{BuNH}_2,\ \text{MeNH}_2 \leq \text{4-tbp, py} < {}^t\text{BuNC} < PCy_3 < PPh_3,\ P^nBu_3 \leq PEt_3 \quad (1)$$

Such a qualitative ligand series is not available for mononuclear tungsten complexes, to the best of our knowledge. Furthermore, the substitution behavior of ligands on metal clusters has rarely been correlated with the behavior of single metal complexes. Among the exceptions are Hughbanks and co-workers' studies of $Zr_6Cl_{12}XL_6$ clusters in which the behavior of ligands on those clusters was found to qualitatively agree with the ligand properties of the Zr(IV) complexes.[52] To some extent, the spectrochemical series[53,54] can serve as an approximate guideline to the ligand binding strength, although the parameter that determines that sequence does not exactly reflect the thermodynamics of ligand exchange. The ligands studied so far for the W_6S_8 cluster make up only a small section of the spectrochemical series (from NH_3 to PR_3). However, this series is not specific enough to explain the differences observed here. More useful guidelines are the C_B/E_B parameters (ECW model)[54−56] defined and compiled by Drago and co-workers as a quantitative dual parameter scale of basicity for σ donors. The good ligands reported to date all have a fairly large covalency parameter (C_B, listed in Table 1), which is always greater than 3, while the nonbinding "solvents" such as benzene, DMF, THF, DMSO, acetonitrile, and benzonitrile have C_B values smaller than 2. High E_B values of ligands do not appear to be as important in ligand binding to these W_6S_8 clusters. On the basis of its preferences for ligands with large covalency parameters, the W_6S_8 cluster appears to be "soft" and "covalent" (as opposed to "hard" and "electrostatic"). The difference between amines still cannot be readily explained by these parameters alone. Piperidine, diethylamine, and tertiary amines all have higher C_B than 4-tbp, yet they are less strongly bound or do not bind at all. Perhaps this is the consequence of the steric repulsion, which is not reflected in the ECW model[44,56] and quite pronounced in the cases of the cluster compounds compared with the metal ions traditionally studied.

B. Crystal Structures. The crystal structures for the new $W_6S_8L_6$ clusters were solved. Their molecular structures are shown in Figure 2. Selected bond lengths and angles are listed in Table 5 (see Supporting Information for more details). All complexes share the same W_6S_8 core structure, which can be described as an octahedron of tungsten atoms with their octahedral faces capped by eight triply bridging sulfur atoms. The W_6S_8 octahedra in all complexes are quite regular, as evidenced by the small variations of bond lengths and angles (see Table 5) despite the low imposed symmetries (inversion centers for all but **2**, which is the asymmetric unit). Six donor ligands L coordinate to the six W atoms. The different axial ligands lead to some small metric variations, which will be the emphasis of the discussion.

There are two features worth mentioning before the discussion of the metric features. In the structure of **6**, the ligand *tert*-butyl groups have much conformational freedom; in the other observed crystal structure (space group $P\bar{3}1c$), some of the *tert*-butyl groups are oriented differently to accommodate a packing scheme without solvents of crystallization. The C−N−C bond angles in the isocyanide complex (**3**) are 178.6°, 174.5°, and 170.3°. These nearly linear angles, as opposed to the occasional observed bent C−N−C angles, indicate single metal−ligand bonds (W−C≡N).[53]

The average W−W distances are 2.676(2), 2.683(4), 2.681(3), 2.662(5), 2.661(8), and 2.664(3) Å for $W_6S_8L_6$ clusters with L = P^nBu_3 (**1**), PPh_3 (**2**), ^{t}BuNC (**3**), morpholine (**4**), $MeNH_2$ (**5**), and ^{t}BuNH$_2$ (**6**), respectively. Among them, the average W−W distance in the PPh_3 cluster is the longest and the one in the methylamine cluster is the shortest. They are within the range observed in previously known $W_6S_8L_6$ clusters. On the basis of Pauling's relation[57] and the single bond distance of 2.635 Å for W,[58] the bond orders of these W−W average

(52) Xie, X.; Reibenspies, J. H.; Hughbanks, T. *J. Am. Chem. Soc.* **1998**, *120*, 11391−11400.
(53) Cotton, F. A.; Wilkinson, G.; Bochmann, M.; Murillo, C. *Advanced Inorganic Chemistry*, 6th ed.; Wiley: New York, 1998.
(54) Shriver, D. F.; Atkins, P. W.; Langford, C. H. *Inorganic Chemistry*, 2nd ed.; W. H. Freeman and Company: New York, 1996.
(55) Huheey, J. E.; Keiter, E. A.; Keiter, R. L. *Inorganic Chemistry*: *Principles of Structure and Reactivity*, 4th ed.; HarperCollins College Publishers: New York, 1993.
(56) Vogel, G. C.; Drago, R. S. *J. Chem. Educ.* **1996**, *73*, 701−707.

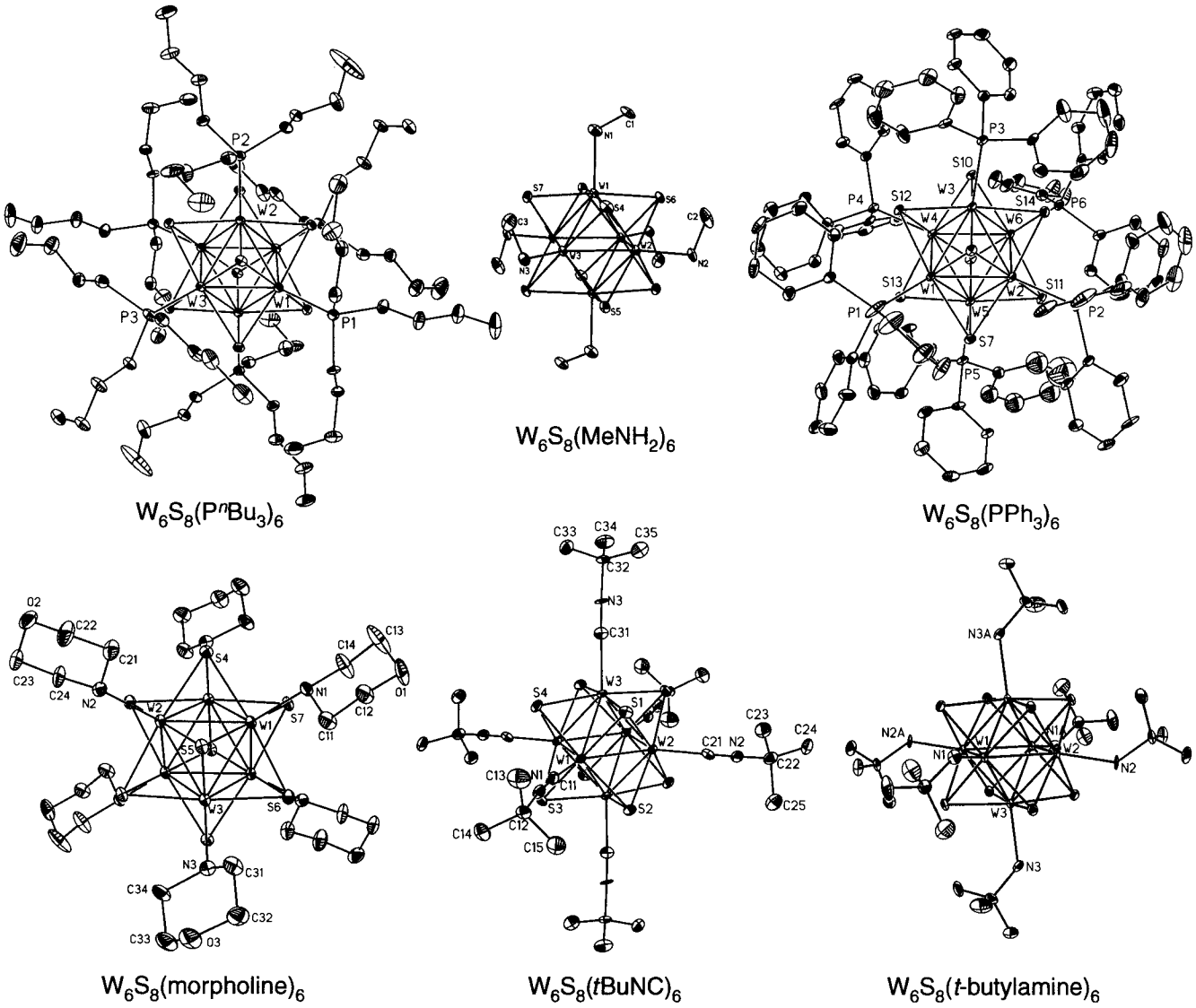

Figure 2. ORTEP drawings of $W_6S_8(P^nBu_3)_6$ (**1**), $W_6S_8(PPh_3)_6$ (**2**), $W_6S_8(^tBuNC)_6$ (**3**), W_6S_8(morpholine)$_6$ (**4**), $W_6S_8(MeNH_2)_6$ (**5**), and W_6S_8(*tert*-butylamine)$_6$ (**6**) clusters with partial labeling schemes. Thermal ellipsoids are shown at the 30% probability level except for **5**, which is at 50%. Hydrogen atoms are omitted for clarity.

distances are calculated as 0.854, 0.833, 0.838, 0.902, 0.906, and 0.896 for **1**−**6**, respectively, which are close to the expected bond order of $^{20}/_{24} = 0.833$ for 20 e clusters.

The average W−P distances in **1** (2.518(1) Å) and W−N distances in **4**, **5**, and **6** (2.307(4), 2.278(11), and 2.303(8) Å, respectively) are comparable to values previously reported, such as for clusters **7**, **11**, and **13** (see Table 6). The average W−P distance in **2** (2.570(12) Å) is slightly longer than the W−P distances in phosphine clusters **7** (2.521 Å) and **1** but still shorter than that of **8** (2.604 Å). Also, the W−P bonds in **2** are not perpendicular to the square S faces of the W_6S_8 cluster, and the PPh_3 ligands lean over the phenyl rings that are most parallel to the cluster faces (see Figure S2 in Supporting Information). This results in a relatively large distortion of the nominal octahedron of the ligands (see δ_{L-L} in Table 5). These effects are due to steric repulsion between the bulky PPh_3 ligands and the S atoms on each face of the cluster cube. The W−C distance in **3** (2.160(10) Å) is close to that found in the mononuclear tungsten isocyanide complexes $[(^tBuNC)_7W]^{2+}$ (2.06(2)−2.12(2) Å), which has a similar oxidation state (+II) for W.[59] However, to compare the W−L distances with different ligands, we have to turn our attention to the W−S bonds first. The average W−S distances are 2.458(4), 2.449(12), 2.450(5), 2.458(5), 2.462(15), and 2.464(9) Å for clusters **1**−**6**, respectively, and are relatively insensitive to the different axial ligands. This near constancy was reported by McCarley and co-workers based on a limited comparison and was used to estimate the covalent radius of the W atom.[18] With 13 $W_6S_8L_6$ structures known to date, the W−S distance is found to be indeed quite insensitive to the ligand environment. The average W−S bond distance is 2.455 Å with a maximum deviation of 0.016 Å for the average of all complexes and a maximum deviation of 0.055 Å for all W−S bonds. Following McCarley, we use this average

(57) Pauling, L. *The Nature of the Chemical Bond*; Cornell University Press: Ithaca, NY, 1960.
(58) Pearson, W. B. *The Crystal Chemistry and Physics of Metals and Alloys*; Wiley: New York, 1972.
(59) LaRue, W. A.; Anh Thu, L.; San Filippo, J., Jr. *Inorg. Chem.* **1980**, *19*, 315−320.

Table 6. Summary of Structural and TGA Data for $W_6S_8L_6$ Complexes[a]

ligand L	W−W (Å)	BO[b] (W−W)	W−L (Å)	BO[c] (W−L)	TGA[d] (°C)	ref
PEt_3	2.680	0.841	2.521	0.985	250	21
P^nBu_3	2.676	0.854	2.518	0.996	220	here
PPh_3	2.683	0.833	2.570	0.816	240	here
PCy_3	2.684	0.829	2.604	0.716	230	23
^{t}BuNC	2.681	0.838	2.160	1.118	170	here
THT	2.653	0.933	2.548	0.68	200	15
4-tbp	2.662	0.902	2.257	0.584	190	16
py	2.662	0.902	2.263	0.571	180	16
$MeNH_2$	2.661	0.906	2.278	0.539	160	here
^{n}BuNH$_2$	2.655	0.926	2.27	0.556	100	23
pip	2.666	0.888	2.312	0.473	150	21
morph	2.662	0.902	2.307	0.482	125	here
^{t}BuNH$_2$	2.664	0.896	2.303	0.490	140	here

[a] Ligands are organized according to the thermodynamic series based on the exchange studies. THT was not subjected to ligand exchange studies but is placed according to the W−L bond order. [b] BO (W−W) (bond order of W−W) n is defined as $d(n) = d(1) - 0.6 \log n$, where $d(1) = 2.635$ Å for W (refs 56 and 57). [c] BO (W−L) (bond order of W−L) n is defined as $d(n) = d(1) - 0.6 \log n$, where $d(1) = r(W) + r(L)$ (see text). [d] TGA decomposition temperatures (indicated by the onset of weight loss of the ligands) of the corresponding $W_6S_8L_6$ cluster compounds.

W−S distance to compute the bond order of W−L bonds.

$$r(W) = d(W-S) - r(S) = 2.455 - 1.04 = 1.415\ (Å)$$

$$d(W-P)_{cal} = r(W) + r(P) = 1.415 + 1.10 = 2.515\ (Å)$$

$$d(W-N)_{cal} = r(W) + r(N) = 1.415 + 0.70 = 2.115\ (Å)$$

$$d(W-C)_{cal} = r(W) + r(C) = 1.415 + 0.772 = 2.187\ (Å)$$

The W−L bond orders are 0.988 and 0.810 for the W−P bond in **1** and **2**, respectively, 1.111 for the W−C bond in **3**, and 0.479, 0.535, and 0.486 for the W−N bonds in clusters **4**, **5**, and **6**, respectively. These and other bond orders calculated for $W_6S_8L_6$ clusters are collected in Table 6, in which the ligands are organized according to the thermodynamic series based on the ligand exchange studies (series 1). The W−L bond orders roughly follow a trend with a pronounced exception: ^{t}BuNC. The average W−W distances and bond orders for these clusters were also listed in Table 6. Despite the small differences, the division of these distances into two groups is still obvious. The first group includes the phosphines and isocyanide, and they have W−W bond orders around 0.84. The second group has a W−W bond order around 0.90. This division is in agreement with the observation of ligand exchange reactions; phosphines and isocyanides are strongly bound to the clusters, while the amines are in general weaker. The inverse correlation between W−L bond order and W−W distance can be explained by a simple bond valence consideration. An increase in the W−L bond order decreases the bond order of the W−W bond so that the total valence sum is maintained.

C. Thermogravimetric Analysis (TGA). Thermogravimetric analyses (TGA) of the clusters can also give an approximate indication of the binding strength and/or lability of the ligands. It was observed that thermal deligation occurs under TGA conditions and the volatile free ligand is carried away by the flow gas, leaving amorphous products.[15,21] The thermal loss of strongly bound ligands should be more difficult than that of weakly bound ligands, although the behavior of the solid/gas decomposition reaction under nonequilibrium conditions (heating rates of 20 °C/min and under flowing gas) may be different from ligand exchange reactions in solutions. The kinetics of mass loss with the TGA are affected by a number of factors: the ligand binding energy, the vapor pressure of the free ligands, the strong confinement effects on a ligand by the surrounding solid-state lattice, and the crystallinity and particle size of the samples. Yet one might expect some correlation between the onset of mass loss in TGA and the relative free energies of ligand binding as determined by ligand exchange reactions. The TGA traces of the new complexes reported herein are shown in Figure 3. In the cases of complexes **2**, **4**, and **5**, the volatile compounds lost from the samples were confirmed by TGA−mass spectrometry to be the corresponding free ligands. Compound **3** has benzene as the solvent of crystallization as prepared and slowly loses the solvent at lower temperature. The decomposition temperatures of these cluster complexes (T_d, indicated by the onset of weight loss of the ligands) are listed in Table 6 along with those reported previously.

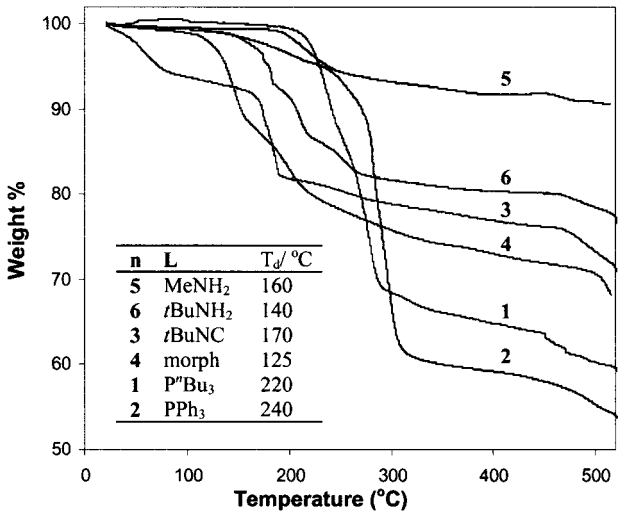

Figure 3. TGA traces of the cluster complexes **1**−**6** presented on the same vertical scale of percentage weight loss. The decomposition temperatures (T_d, indicated by the onset of weight loss of the ligands) are listed in the inset table.

A TGA ligand series based on the decomposition temperatures (T_d) of the corresponding clusters is

$$^n\text{BuNH}_2 < \text{morpholine} < {}^t\text{BuNH}_2 < \text{pip} < \text{MeNH}_2 < {}^t\text{BuNC} < \text{py} < \text{4-tbp} < \text{THT} < \text{P}^n\text{Bu}_3 < \text{PCy}_3 < \text{PPh}_3 < \text{PEt}_3 \quad (2)$$

The T_d does not follow the exact order of the thermodynamic series or the bond order. Nevertheless, a rough trend holds: clusters with phosphine ligands have higher T_d's, and clusters with amines have lower T_d's. In general, the more strongly bound the ligand L, the higher is the T_d for that cluster.

D. Kinetic Aspects. Throughout the discussion so far, equilibrium results have been sought, but the kinetics of the ligand exchanges were largely overlooked as long as the equilibrium was guaranteed under the reaction conditions applied (100 °C for at least a day), which was always the case. Nevertheless, some qualitative differences in the lability of the ligands were observed. Cluster complexes with alkylamine ligands such ^{n}BuNH$_2$ and ^{t}BuNH$_2$ undergo significant ligand exchange with other ligands at room temperature; at 50 °C such reactions are complete within hours. But a cluster with 4-tbp ligand has to be heated above 50 °C to see any changes at all. For clusters with phosphine ligands, heating at 100 °C for at least a day is often essential for reaching equilibrium. TGA data

also reflect some sign of the kinetics. Weight loss at low temperature is possible only if the dissociative kinetics are rapid at such temperature. In this sense, TGA results qualitatively agree with the observations in the ligand exchange reactions. It also appears that those $W_6S_8L_6$ clusters with thermodynamically more stable ligands are often more inert and those with less stable ligands are often more labile. To evaluate the kinetics of ligand loss or exchange in an accurate manner and to determine the operative mechanism, more detailed systematic studies are needed.

Conclusions

Ligand substitution reactions of $W_6S_8L_6$ clusters were investigated extensively for many ligands. A thermodynamic series of ligand binding strength on the W_6S_8 clusters is established as following:

non-Lewis base solvents, aniline, P^tBu_3, etc. $\ll$ Et_2NH, Bu_2NH $<$ ^{t}BuNH$_2$ $<$ morpholine, pip $\leq$ ^{n}BuNH$_2$, MeNH$_2$ $\leq$ 4-tbp, py $<$ ^{t}BuNC $<$ PCy_3 $<$ PPh_3, P^nBu_3 $\leq$ PEt_3

Six new cluster compounds were synthesized, and their properties were examined with structural and thermogravimetric analyses. These complexes and the associated exchange data are the material base for the rational design of cluster-linking reactions.

Acknowledgment. This work was supported by the Department of Energy (Grant DE-FG02-87ER45298). This work made use of the Polymer Characterization Facility of Cornell Center for Materials Research supported through the NSF Material Research Science and Engineering Centers program (Grant DMR-0079992). We thank Dr. Julie K. Lorenz at Rohm and Haas Co. for performing the TGA−MS analyses.

Supporting Information Available: Lists of atomic positions and parameters, tables of bond lengths and angles for crystal structures of $W_6S_8(P^nBu_3)_6$, $W_6S_8(PPh_3)_6\cdot C_6H_6$, $W_6S_8(^t\text{BuNC})_6\cdot 4C_6H_6$, W_6S_8(morpholine)$_6\cdot$3.7(aniline)$\cdot$1.3(morpholine), $W_6S_8(MeNH_2)_6$, and $W_6S_8(^t\text{BuNH}_2)_6\cdot 2^t\text{BuNH}_2$, experimental and simulated power diffraction patterns for $W_6S_8(MeNH_2)_6$, additional structural diagrams of the $W_6S_8(PPh_3)_6$ cluster to illustrate the ligand distortion, and X-ray crystallographic files in CIF format for the structure determinations of $W_6S_8(P^nBu_3)_6$, $W_6S_8(PPh_3)_6\cdot C_6H_6$, $W_6S_8(^t\text{BuNC})_6\cdot 4C_6H_6$, W_6S_8(morpholine)$_6\cdot$3.7(aniline)$\cdot$1.3(morpholine), $W_6S_8(MeNH_2)_6$, and $W_6S_8(^t\text{BuNH}_2)_6\cdot 2^t\text{BuNH}_2$. This material is available free of charge via the Internet at http://pubs.acs.org.

IC001314Q